Preliminary Analysis of Gaofen-1 B/C/D Satellite Stereo Mapping Performance

Liping Zhao and Xianhui Dou

Abstract The Gaofen-1 (GF-1) B/C/D is optical satellite with two 2/8 m spatial resolution panchromatic/multispectral cameras, and they were launched in March 2018 on a CZ-4C rocket. This paper used the GF-1 B/C/D and Ziyuan-3 (ZY-3) data that had been repeatedly visited in Northeast China to carry out mapping performance research. According to the sensor parameters and imaging geometric model, the instantaneous field of view at different side angles was analyzed, and the influence of ground control data error on image adjustment accuracy was simulated. Then, using the GF-1 B/C/D and ZY-3 data acquired simultaneously, multiple stereo models were constructed. Based on high-precision ground reference dataset, a large number of ground control points were automatically extracted for each stereo model, and then the affine model in image space and the provided rational polynomial coefficients were used for the adjustment. The results show that the root-mean-square error of the elevation of the GF-1 B/C/D stereo models is about 2–3 m. Subsequently, using these stereo models, the digital surface model (DSM) was extracted and analyzed. In general, whether it is the accuracy of stereo model or the performance of DSM extracted, it could meet the 1:50,000 scale mapping specification requirements. However, it is found that some inter-chip stitching errors between CCDs cannot be ignored in the GF-1 B/C/D image data, "elevation fracture" and abnormal elevation values are obvious in the DSM, and these defects need continuous improvement.

Keywords Gaofen-1 B/C/D · ZY-3 · Stereoscopic · Accuracy · DSM

1 Introduction

The Gaofen-1 (GF-1) B/C/D is a Chinese civilian optical satellite with two 2/8 m spatial resolution panchromatic/multispectral cameras. They were launched at a time in March 2018 on a CZ-4C carrier rocket from China's Taiyuan Satellite Launch Center. The three satellites are operated in a same sun-synchronous orbit, but are phased

L. Zhao (✉) · X. Dou
Land Satellite Remote Sensing Application Center, Ministry of Nature Resource, Beijing, China
e-mail: zhaolpwww@163.com

L. Wang et al. (eds.), *Proceedings of the 6th China High Resolution Earth Observation Conference (CHREOC 2019)*, Lecture Notes in Electrical Engineering 657,
https://doi.org/10.1007/978-981-15-3947-3_10

at 120° and an altitude of 645 km, with a 10:30 AM equator crossing time and high revisit frequency of 15 days. The satellites have a ±32° side-swing capability, which could combine multi-sensor data to construct the along- or across-track stereo image pair with different base–height ratios for digital surface model (DSM) extraction.

The Ziyuan-3 (ZY-3) satellite is mainly devoted to the operational services of 1:50,000 scale stereo mapping. The triplet stereoscopic instrument on the ZY-3 is dedicated to simultaneous stereo pair acquisition along the track. Among them, two cameras point to the forward (FWD) and backward (BWD), respectively, at a tilted angle of 22°, and the third points to the nadir (NAD). The satellite also has a lateral viewing capability around the roll axis.

The geometric performances are an important topic for many applications [1–3]. Although stereo mapping was not the design purpose of GF-1 B/C/D, satellites with side view imaging capability could be used for stereo mapping. In this study, the GF-1 B/C/D panchromatic (PAN) data was used in conjunction with ZY-3 image to construct the stereo model. The adjustment scheme based on the affine transformation in the image was used for accuracy analysis. Further, digital surface model (DSM) extraction and comparative analysis were performed using each stereo model.

2 Data

In order to carry out the GF-1 B/C/D stereo mapping performance analysis, this paper uses GF-1 B/C/D and ZY-3 stereo data to construct the multi-source stereo pairs. Table 1 gives the main characteristics of the GF-1 B/C/D and ZY-3. Considering that optical data acquisition is greatly affected by seasonal and weather factors, in order to obtain the best possible data in the same experimental area, the Harbin experimental area in Northeast China is selected for research in this paper. In the region, the main topographic features are flat, with a height difference of less than 60 m. Such flat terrain facilitates the extraction of tie points between images, which could eliminate the influence of terrain as much as possible, and is more conducive to the geometric performance analysis of the image itself.

Between November 1 and 28, 2018, GF-1 B/C/D and ZY-3 01/02 passed through the test area several times with small-angle swaying and successfully obtained data.

Table 1 Main characteristics of the GF-1 B/C/D and ZY-3 (specification)

Satellite	GF-1 B/C/D	ZY-3(01)	ZY-3(02)
Launch periods	March 2018	January 2012	May 2016
Altitude (km)	645	505	505
Cycle (days)	41	59	59
Swath (km)	60	50	50
Mean GSD (m)	PAN: 2.0 m	NAD: 2.1 BWD: 3.5 FWD: 3.5	NAD: 2.1 BWD: 2.5 FWD: 2.5

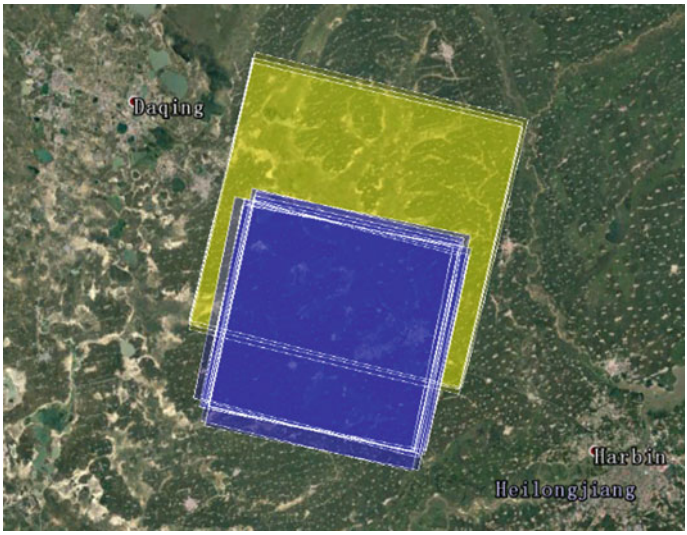

Fig. 1 Test data distribution diagram

Six times of the data were selected according to the test requirements, and the coverage was shown in Fig. 1. Among them, on November 1, 2018, GF-1C and ZY-3 (02) obtained quasi-synchronized data. On November 16, 2018, GF-1B and ZY-3 (02) also transited the test area almost simultaneously. On November 27 and 28, 2018, respectively, GF-1D and ZY-3 (01) successfully obtained data again, and the time difference was one day.

The triplet stereoscopic data of the ZY-3 has two functions. One is to construct the stereo pair with GF-1B/C/D to analyze the mapping performance, and the other is as comparative stereo model data.

As shown in Tables 2 and 3, according to the imaging date, all test data is divided into 3 groups, and each group of data constitutes 5 stereo pairs. Since the above data is obtained by the small-angle side-swing method, in addition to the ZY-3 stereo composed of BWD and FWD, the other stereo pairs constructed have a base-to-height ratio of about 0.44–0.50.

In order to analyze GF-1B/C/D stereo mapping performance, this paper uses two kinds of reference data: One is the traditional high-precision digital ortho-image map (DOM) and digital surface model (DSM) data (referred to as reference DOM and DSM), and the other reference data is the ground three-dimensional (3D) data extracted by the free network adjustment method based on ZY-3 triplet stereo data (referred to as reference ZY-3 3D). In this paper, the horizontal datum and ellipsoidal height of WGS84 are used unless otherwise specified.

Table 2 Main characteristics of the test data

Group	Satellite	Sensor	Date	Time	Roll
Group_B	GF-1B	PAN	20181116	10:50:32	3.925
	ZY-3(02)	NAD	20181116	10:47:40	−5.587
		BWD	20181116	10:48:10	−5.587
		FWD	20181116	10:47:11	−5.587
Group_C	GF-1C	PAN	20181101	10:50:07	3.556
	ZY-3(02)	NAD	20181101	10:52:44	4.165
		BWD	20181101	10:53:13	4.165
		FWD	20181101	10:52:15	4.165
Group_D	GF-1D	PAN	20181127	10:53:14	7.270
	ZY-3(01)	NAD	20181128	10:30:07	−0.007
		BWD	20181128	10:30:36	−0.007
		FWD	20181128	10:29:38	−0.007

Table 3 Stereo models based on GF-1 B/C/D and ZY-3

Group	Satellite	Left image	Right image	Abbreviation
Group_B	GF-1B ZY-3(02)	GF-1B PAN	ZY-3(02) BWD	GF-1B_PB
		GF-1B PAN	ZY-3(02) FWD	GF-1B_PF
		ZY-3(02) NAD	ZY-3(02) BWD	ZY-3(02)_NB_B
		ZY-3(02) NAD	ZY-3(02) FWD	ZY-3(02)_NF_B
		ZY-3(02) BWD	ZY-3(02) FWD	ZY-3(02)_BF_B
Group_C	GF-1C ZY-3(02)	GF-1C PAN	ZY-3(02) BWD	GF-1C_PB
		GF-1C PAN	ZY-3(02) FWD	GF-1C_PF
		ZY-3(02) NAD	ZY-3(02) BWD	ZY-3(02)_NB_C
		ZY-3(02) NAD	ZY-3(02) FWD	ZY-3(02)_NF_C
		ZY-3(02) BWD	ZY-3(02) FWD	ZY-3(02)_BF_C
Group_D	GF-1D ZY-3(01)	GF-1D PAN	ZY-3(01) BWD	GF-1D_PB
		GF-1D PAN	ZY-3(01) FWD	GF-1D_PF
		ZY-3(01) NAD	ZY-3(01) BWD	ZY-3(01)_NB_D
		ZY-3(01) NAD	ZY-3(01) FWD	ZY-3(01)_NF_D
		ZY-3(01) BWD	ZY-3(01) FWD	ZY-3(01)_BF_D

3 Experiments

Before the evaluation, the simulation analyzed the influence of the ground reference data error on the adjustment accuracy. Then, using the reference data, a large number of ground control points (GCPs) were extracted, and image accuracy and stereo model accuracy were analyzed. Finally, DSM extraction and analysis were performed.

3.1 Simulation

In order to obtain prior knowledge of the GF-1 B/C/D and ZY-3 satellite data processing and analysis, based on the specifications of satellite and imaging geometry models, the instantaneous field of view (IFOV) under different lateral viewing angle conditions is presented (Fig. 2), and the simulation analyzes the impact of ground control data error on the adjustment accuracy (Figs. 3, 4, 5, 6, 7 and 8).

It could be seen from Fig. 2 that the small-angle side view has little effect on the IFOV of satellite images such as GF-1 B/C/D. The maximum side angle of the experimental data in this paper is 7.270°, which is negligible. A similar situation is also true for ZY-3.

Analysis of Figs. 3 and 4 shows that the ground reference data planimetric error has a significant impact on the accuracy of the GF-1 B/C/D image. The error of one ground sample distance (GSD) corresponds to one pixel on the image. Therefore, if the error in image space is required to be better than 0.3 pixels, the planimetric accuracy of the ground reference data needs to be at least 0.6 m. It could be seen from Fig. 5 that the influence of the ground data elevation error is related to the position

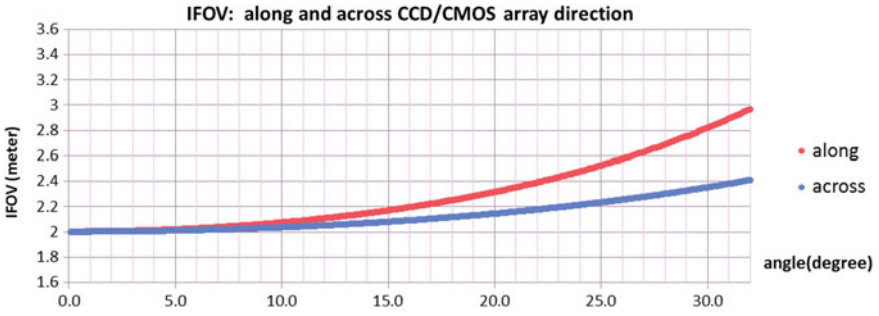

Fig. 2 IFOV with different side views (GF-1 B/C/D PAN)

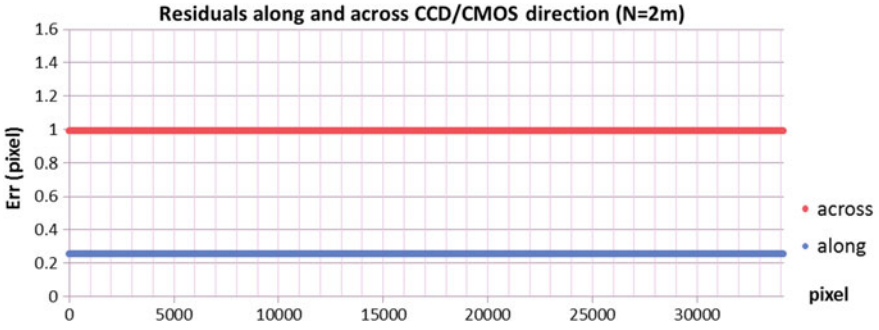

Fig. 3 Influence of ground reference data error on the GF-1 B/C/D PAN image (err_N = 2 m)

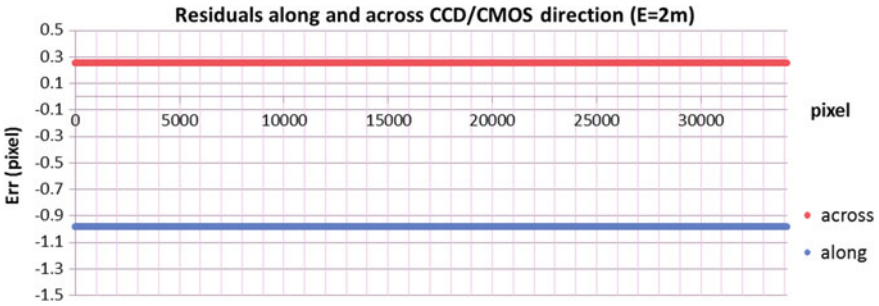

Fig. 4 Influence of ground reference data error on the GF-1 B/C/D PAN image (err_E = 2 m)

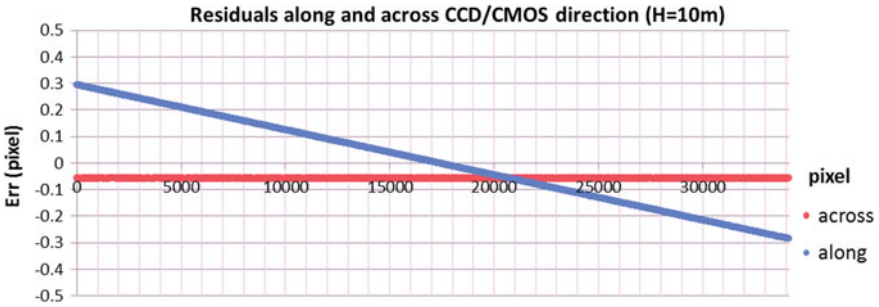

Fig. 5 Influence of ground reference data error on the GF-1 B/C/D PAN image (err_H = 10 m)

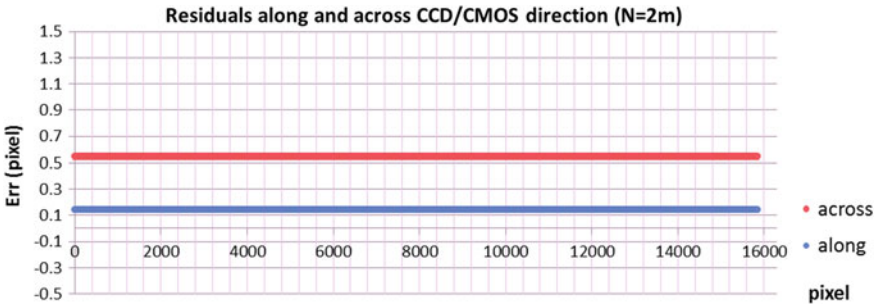

Fig. 6 Influence of ground reference data error on the ZY-3 BWD image (err_N = 2 m)

of the GF-1 B/C/D image in the field of view, and the impact on the adjustment accuracy is small. The effect on the ZY-3 NAD camera is similar.

The ZY-3 BWD and FWD cameras differ from the GF-1 B/C/D PAN cameras in that they have a large angle of inclination along the orbit direction. Taking the ZY-3(01) BWD camera as an example, Figs. 6 and 7 show the influence of the planimetric error and Fig. 8 shows the influence of the elevation error. As could be seen from Figs. 6 and 7, the planimetric error effect is similar to that of the GF-1 B/C/D PAN

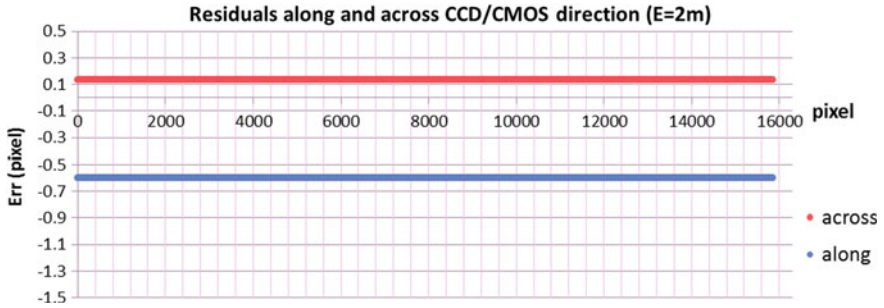

Fig. 7 Influence of ground reference data error on the ZY-3 BWD image (err_N = 2 m)

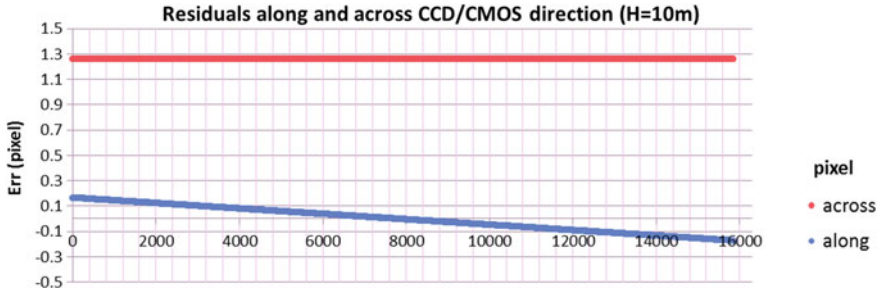

Fig. 8 Influence of ground reference data error on the ZY-3 BWD image (err_H = 10 m)

camera. It could be seen from Fig. 8 that the influence of the elevation error of the ground data in the direction of the line array is negligible, and the influence on the accuracy of the vertical line array direction is very important. Therefore, for the ZY-3 BWD and FWD camera, if the required error in image space is better than 0.3 pixels, the ground reference data planimetric accuracy needs to be better than 1.0 m, and the elevation accuracy needs to be at least 2.5 m, which requires the reference data to have good elevation accuracy.

3.2 GCP Collection

Based on high-precision DOM and DSM data, a large number of GCPs could be automatically acquired by image matching, which is a recommended method. Using this method, on each stereo model, tens of thousands of GCPs could be extracted as needed.

A reference dataset is available over this test area. The dataset is comprised of ortho-image with a GSD of 0.5 m and an accuracy around 0.5 m and digital surface model with a grid of 2 m and an accuracy around 1.0 m.

Table 4 Number of points based on two sets of reference data

Group	Count (reference DOM + DSM)	Count (reference ZY-3 3D)
Group_B	11,982	12,888
Group_C	9862	12,026
Group_D	11,558	14,313

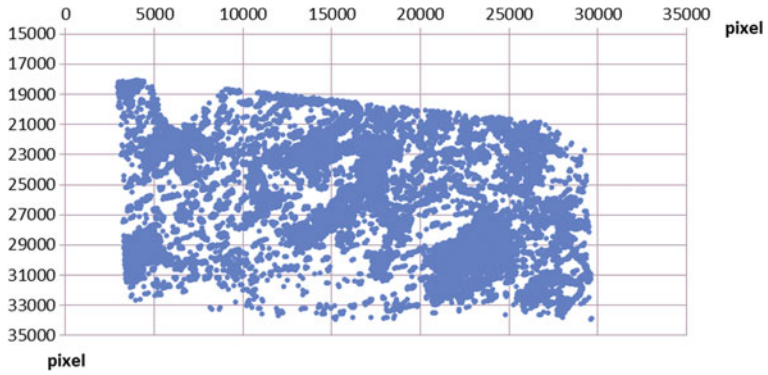

Fig. 9 GCP distribution diagram based on the reference DOM and DSM (Group_B)

Fast Fourier transform phase (FFTP) matching is used to extract tie points due to seasonal differences between the selected test data and the reference data. FFTP works in the frequency domain, it pays more attention to the texture information of the image, and the registration of the multi-temporal image is more robust.

In addition, considering that the ZY-3 stereo model has stable and good precision, the extracted ground planimetric and vertical data based on ZY-3 triplet stereo data is also used as reference data for comparison and analysis. The acquisition time of each group of image data from GF-1 B/C/D and ZY-3 01/02 in this test area is very close, and the land coverage has almost no change. It is very beneficial for extracting tie points between images and has better reliability for analyzing mapping performance.

Table 4 shows the number of GCPs obtained by the two schemes. As for the Group_B data, Figs. 9 and 10, respectively, show the distribution. It could be clearly seen that the GCP distribution of the reference ZY-3 3D is better.

3.3 Adjustment

Rational function model is often used as an imaging geometry model to establish the mapping relationship between image and ground [4, 5]. In the experiments, the vendor-supplied rational polynomial coefficients (RPCs) and affine transformation compensation models in image space are used for accuracy analysis. The ground

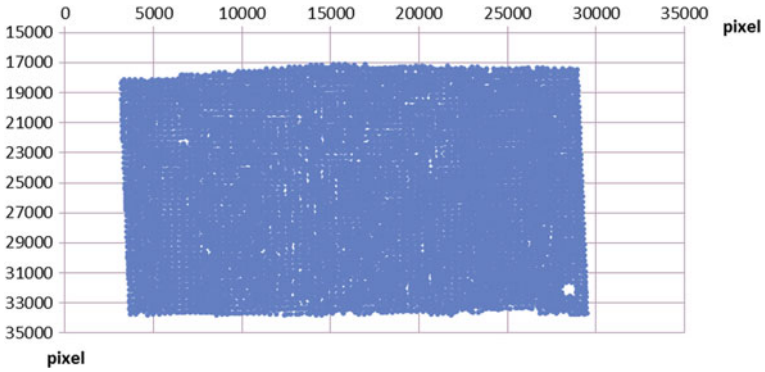

Fig. 10 GCP distribution diagram based on the reference ZY-3 3D (Group_B)

coordinates of the stereo model are calculated by the tie points between the left and right images. The accuracy of the two schemes based on the reference DOM and DSM and reference ZY-3 3D is separately analyzed.

3.3.1 Adjustment with Reference DOM and DSM

According to the conventional method, the adjustment accuracy of the GCPs extracted based on the high-precision reference DOM and DSM dataset is analyzed. Table 5 shows the image accuracy of the GF-1 B/C/D and ZY-3. Taking the data Group_B as an example, the residuals of velocity direction with affine adjustment model on the image of GF-1B and ZY-3 NAD, BWD and FWD are shown in Figs. 11,

Table 5 Image accuracy of the stereo model (unit: pixel)

Group	Sat	Sensor	mSamp	mLine	mPlane
Group_B	GF-1B	PAN	0.611	0.543	0.817
	ZY-3(02)	NAD	0.318	0.318	0.450
		BWD	0.348	0.331	0.481
		FWD	0.309	0.416	0.518
Group_C	GF-1C	PAN	0.569	0.531	0.779
	ZY-3(02)	NAD	0.402	0.499	0.641
		BWD	0.501	0.510	0.715
		FWD	0.373	0.508	0.630
Group_D	GF-1D	PAN	0.458	0.652	0.797
	ZY-3(01)	NAD	0.348	0.364	0.503
		BWD	0.342	0.294	0.451
		FWD	0.286	0.354	0.455

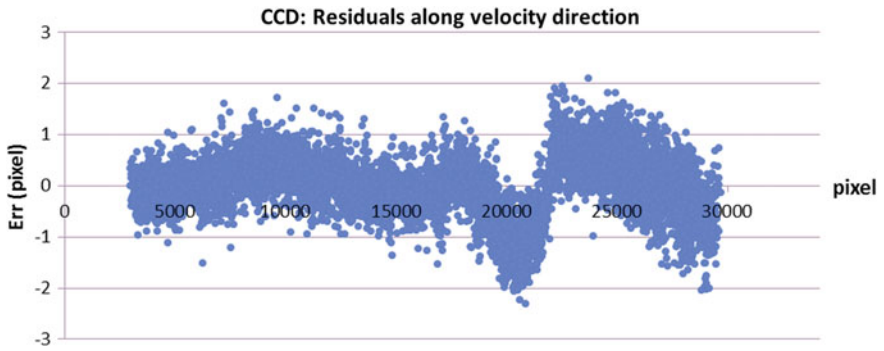

Fig. 11 Residuals of velocity direction with affine adjustment model on the image (GF-1B_20181116)

12, 13 and 14, respectively. In the figure, the abscissa is the sequence number of the pixel, and the ordinate is the residuals. As could be seen from Fig. 11, there are still some minor systematic errors in GF-1B, while the residuals of ZY-3 NAD, BWD and FWD are much smaller (Figs. 12, 13 and 14).

Comparing the data in Table 5, and analyzing Figs. 11, 12, 13 and 14, the following conclusions could be drawn:

- ZY-3 image is more accurate.
- Using ZY-3 data as a reference and comparison data, it is appropriate to perform GF-1 B/C/D accuracy analysis.

Tables 6, 7 and 8 provide a summary of the accuracy of the three sets of data such as Group_B, Group_C and Group_D. It could be seen that the accuracy of each group of data meets the requirements of the 1:50,000 scale stereo mapping specification.

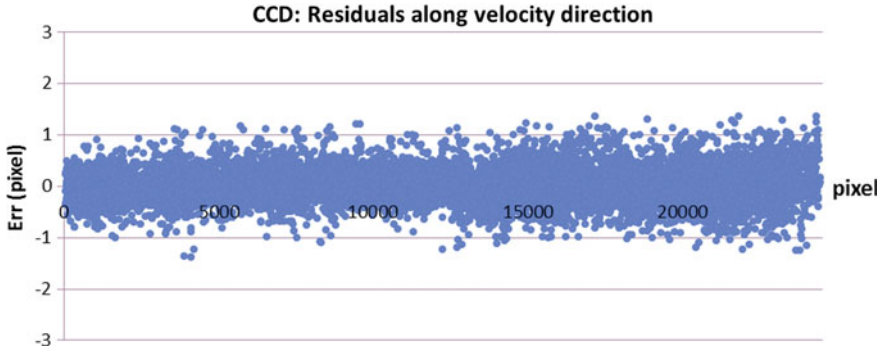

Fig. 12 Residuals of velocity direction with affine adjustment model on the image (ZY-3(02)_NAD_20181116)

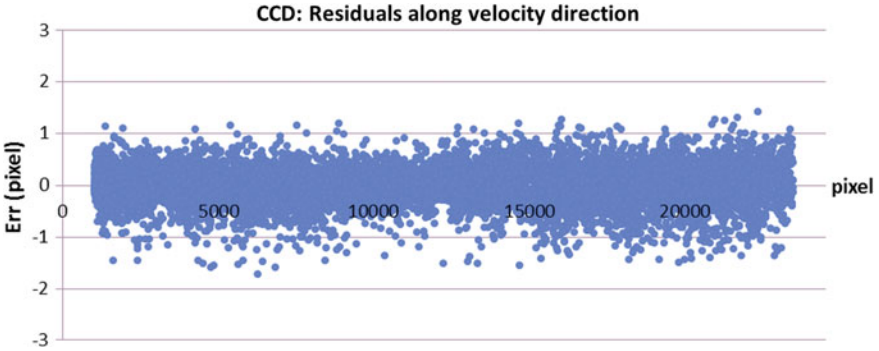

Fig. 13 Residuals of velocity direction with affine adjustment model on the image (ZY-3(02)_BWD_20181116)

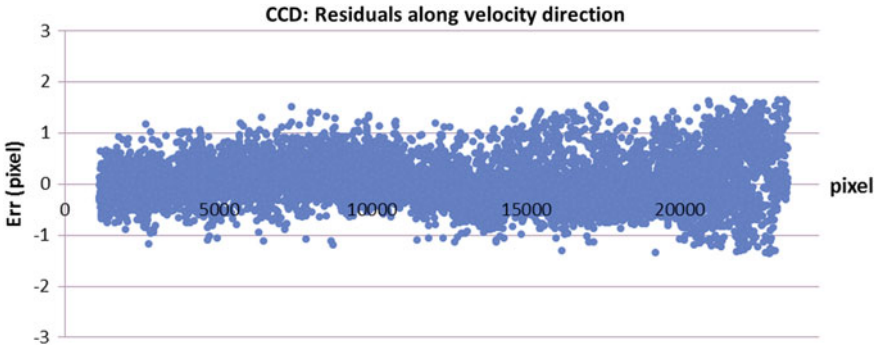

Fig. 14 Residuals of velocity direction with affine adjustment model on the image (ZY-3(02)_FWD_20181116)

Table 6 Ground accuracy of the stereo model (Group_B) (unit: meter)

Stereo model	mN	mE	mH	mH/GSD
GF-1B_PB	1.074	0.863	2.352	0.941
GF-1B_PF	1.020	0.860	2.335	0.934
ZY-3(02)_NB_B	0.691	0.649	1.409	0.564
ZY-3(02)_NF_B	0.678	0.626	1.648	0.659
ZY-3(02)_BF_B	0.808	0.663	1.174	0.470

3.3.2 Adjustment with Reference ZY-3 3D

The GF-1 B/C/D adjustment accuracy analysis based on ZY-3 stereo data is also a good method. Table 9 shows the accuracy in the image space of GF-1 B/C/D, and Table 10 summarizes the accuracy in the object space of Group_B, Group_C and

Table 7 Ground accuracy of the stereo model (Group_C) (unit: meter)

Stereo model	mN	mE	mH	mH/GSD
GF-1C_PB	1.094	0.932	2.305	0.922
GF-1C_PF	1.116	0.833	2.564	1.026
ZY-3(02)_NB_C	1.093	0.918	2.526	1.010
ZY-3(02)_NF_C	1.091	0.733	2.312	0.925
ZY-3(02)_BF_C	1.160	0.855	1.372	0.549

Table 8 Ground accuracy of the stereo model (Group_D) (unit: meter)

Stereo model	mN	mE	mH	mH/GSD
GF-1D_PB	1.236	0.874	2.877	0.822
GF-1D_PF	1.343	0.752	2.516	0.719
ZY-3(02)_NB_D	0.816	0.720	2.011	0.575
ZY-3(02)_NF_D	0.801	0.681	2.056	0.587
ZY-3(02)_BF_D	1.037	0.883	1.426	0.407

Table 9 Image accuracy of the stereo model based on reference ZY-3 3D (unit: pixel)

Group	Sat	Sensor	mSamp	mLine	mPlane
Group_B	GF-1B	PAN	0.717	0.465	0.855
Group_C	GF-1C	PAN	0.451	0.415	0.613
Group_D	GF-1D	PAN	0.354	0.546	0.650

Table 10 Ground accuracy of the stereo model based on reference ZY-3 3D (unit: meter)

Group	Stereo model	mN	mE	mH	mH/GSD
Group_B	GF-1B_PB	0.994	0.751	2.490	0.996
	GF-1B_PF	0.848	0.823	1.845	0.738
Group_C	GF-1C_PB	0.822	0.449	1.846	0.738
	GF-1C_PF	0.916	0.495	2.010	0.804
Group_D	GF-1D_PB	0.982	0.596	2.562	0.732
	GF-1D_PF	1.100	0.495	2.285	0.653

Group_D. Taking GF-1B data as an example, Fig. 15 shows the residuals of velocity direction on the image using affine adjustment model based on reference ZY-3 3D. Overall, the accuracy obtained by this method is similar to that of the method based on the high-precision reference DOM and DSM.

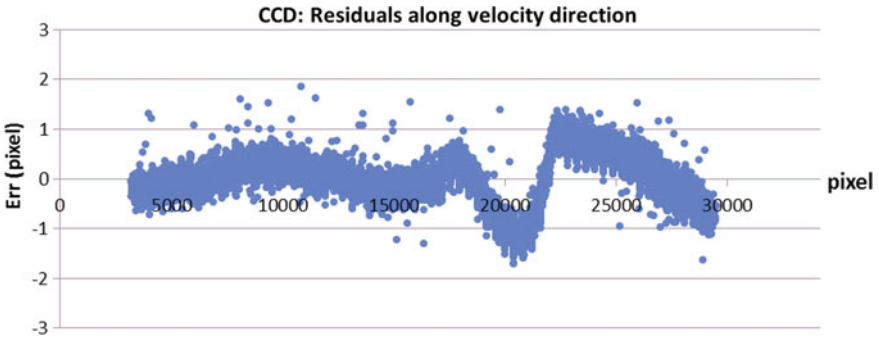

Fig. 15 Residuals of velocity direction on the image using affine adjustment model based on reference ZY-3 3D (GF-1B_20181116)

3.4 DSM Generation and Comparison

After adjustment with the GCPs, the DSM had been generated with a grid spacing of 5 m. For comparative analysis, all DSMs were extracted using the same methods and parameters, without any manual interaction editing. For the stereo image model GF-1B_PB, which is constructed by GF-1B_PAN_20181116 and ZY-3(02)_BWD_20181116 images, Fig. 16 shows the overall shading of the DSM, and more DSM details could be found in the partial shading map of sites B1, B2 and B3 (Figs. 18, 19 and 20). As a comparative stereo model ZY-3(02)_NB_B, which consists of ZY-3(02)_NAD_20181116 and ZY-3(02)_BWD_20181116 images, the corresponding shading maps are given in Figs. 17, 18, 19 and 20, respectively.

Analyzing Figs. 18, 19 and 20, compared with the DSM extracted based on the ZY-3 stereo model, it could be clearly seen that the DSM based on model GF-1B_PB has the following problems:

- Poor detail performance.
- There is an abnormal "elevation fracture" at about 1/3 of the right side, which corresponds to the image residual distribution map shown in Figs. 11 and 15.
- There are more abnormal elevation values in some residential areas and road areas.

In addition, the DSM extracted by other stereo models constructed by GF-1 B/C/D is similar to the DSM from GF-1B_PB, and details are not discussed herein. In terms of DSM extraction, although there are some problems with the automatically extracted DSM, after manual processing, in most cases, the accuracy and quality could meet the 1:50,000 scale mapping specification requirements.

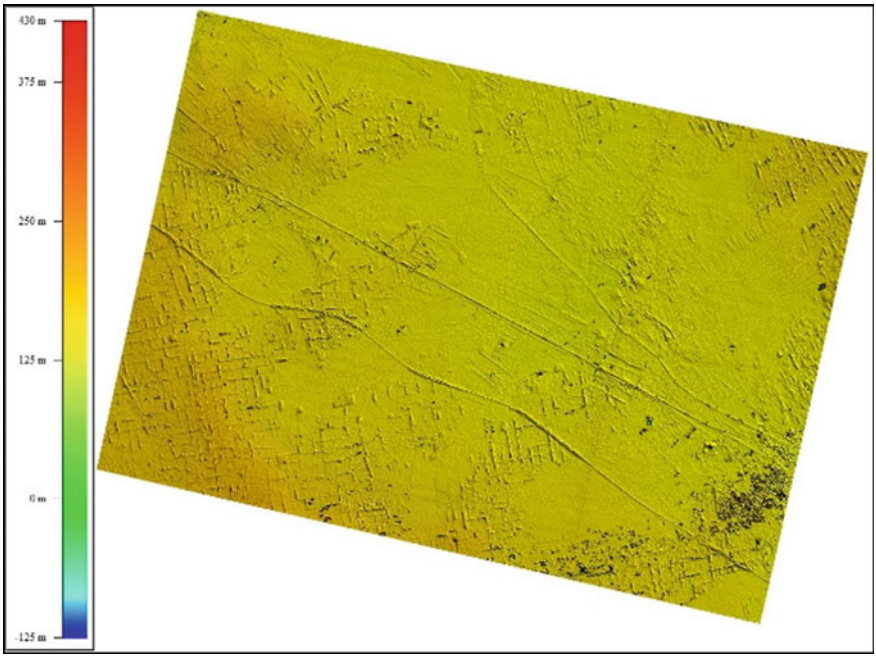

Fig. 16 DSM shaded map from the stereo GF-1B_PB

4 Conclusion

For the Chinese civil GF-1 B/C/D satellites, this paper selected the data of repeated visits in Northeast China and initially carried out the evaluation and analysis of the stereo mapping performance. The ZY-3 mapping satellite data acquired simultaneously was used for comparative analysis.

The affine model in image space and the provided RPC were used for the adjustment calculation. The experimental results show that the root-mean-square error of the elevation of the GF-1 B/C/D stereo model is about 2–3 m, compared with ZY-3, and its accuracy and the performance of DSM extracted by it are slightly worse, but they all meet the 1:50,000 scale mapping specification.

Through analysis of image adjustment residuals and the DSM extracted by the stereo model, it was found that some inter-chip stitching errors between CCDs were obvious in the GF-1B/C/D image data, and it was necessary to continue the refined geometric calibration to reduce the stitching errors.

As far as DSM extraction was concerned, it was found that DSMs automatically extracted by the GF-1 B/C/D stereo model had obvious “elevation fracture” and abnormal elevation values. Especially for artificial buildings and roads, the DSM had many defects and requires manual interactive editing to improve quality.

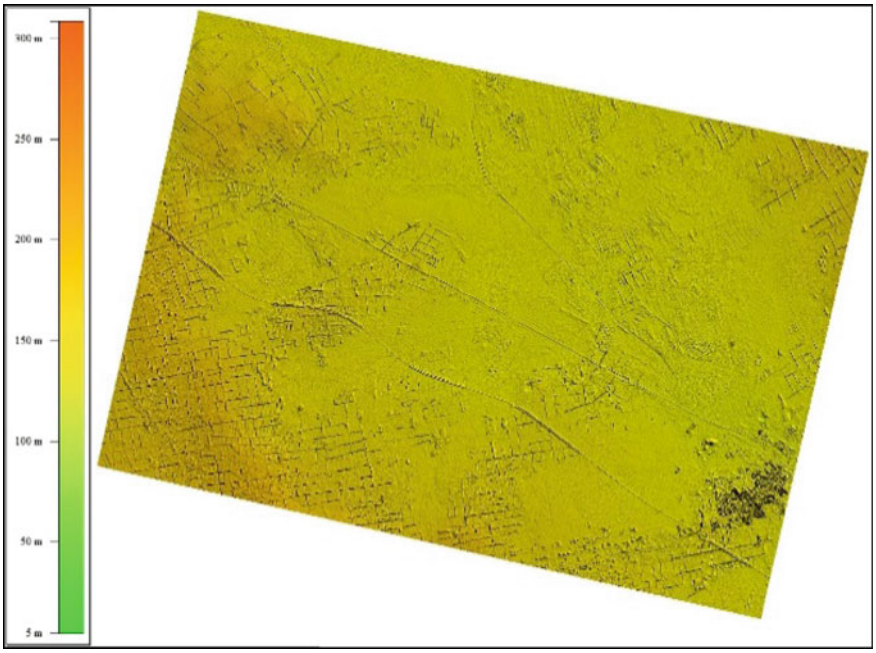

Fig. 17 DSM shaded map from the stereo ZY-3(02)_NB_B

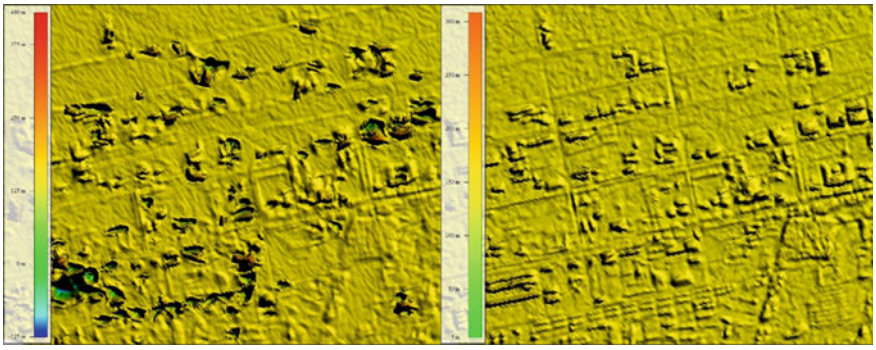

Fig. 18 DSM shaded map of site B1 from the stereo GF-1B_PB and ZY-3(02)_NB_B (left: GF-1B_PB, right: ZY-3(02)_NB_B)

In general, although the GF-1 B/C/D satellite was not designed for mapping, the data could still be used for stereo mapping. Continuous improvement was necessary for some of the shortcomings that currently exist.

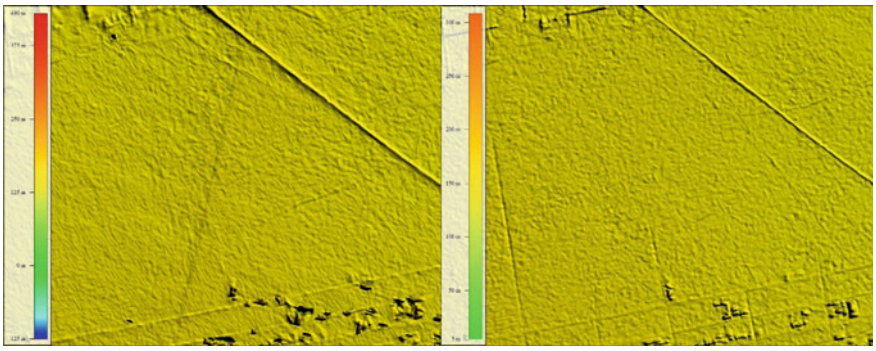

Fig. 19 DSM shaded map of site B2 from the stereo GF-1B_PB and ZY-3(02)_NB_B (left: GF-1B_PB, right: ZY-3(02)_NB_B)

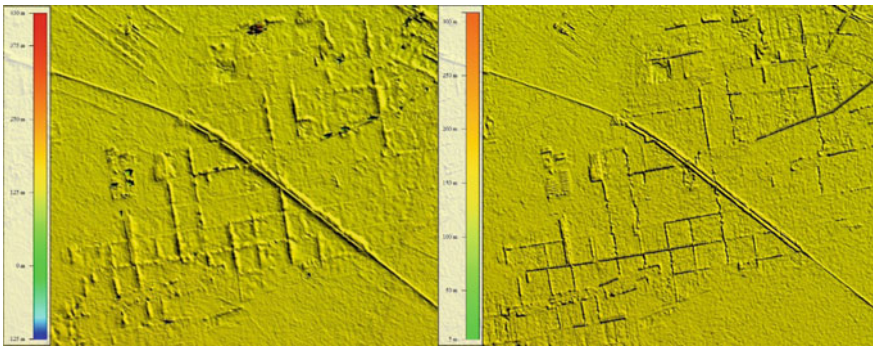

Fig. 20 DSM shaded map of site B3 from the stereo GF-1B_PB and ZY-3(02)_NB_B (left: GF-1B_PB, right: ZY-3(02)_NB_B)

References

1. Jacobsen K (2016) Analysis and correction of systematic height model errors. Int Arch Photogramm Remote Sens Spatial Inf Sci XLI-B1:333–339
2. Jacobsen K (2017) Problems and limitations of satellite image orientation for determination of height models. Int Arch Photogramm Remote Sens Spatial Inf Sci XLII-1/W1:257–264
3. Jacobsen K (2018) Systematic geometric image errors of very high resolution optical satellites. Int Arch Photogramm Remote Sens Spatial Inf Sci XLII-1:233–238
4. Grodecki, J (2001) IKONOS stereo feature extraction—RPC approach. In: ASPRS annual conference, St. Louis
5. Grodecki J, Dial G (2003) Block adjustment of high-resolution satellite images described by rational functions. Photogramm Eng Remote Sens 69:59–70